

## LARGE TRANSVERSE MOMENTUM PHOTONS FROM HIGH-ENERGY PROTON-PROTON COLLISIONS

P. DARRIULAT, P. DITTMANN, K. EGGERT <sup>\*</sup>, M. HOLDER,  
K.T. McDONALD <sup>\*\*</sup>, T. MODIS <sup>\*\*\*</sup>, F.L. NAVARRIA <sup>†</sup>, A. SEIDEN <sup>††</sup>,  
J. STRAUSS, G. VESZTERGOMBI <sup>†††</sup> and E.G.H. WILLIAMS  
*CERN, Geneva, Switzerland*

Received 9 June 1976

We have performed a simultaneous measurement of the large transverse momentum (1.6 to 3.8 GeV/c) yields of single photons and of photon pairs at 90° production angle in pp collisions at ISR energies. Production cross sections for each of these two processes are compared.

### 1. Introduction

Large transverse momentum production of photons from pp collisions has been the object of many investigations both at FNAL [1] and at the ISR [2,3]. Such experiments have used lead glass detectors [4,5] which permit detection of photons over a large solid angle, with good resolutions in energy and in position. However, no systematic investigation concerning the source of the observed photons has been made and it has been generally assumed that they are the products of  $\pi^0$  or  $\eta$  decays.

It has recently been argued [6] that quark parton models can accommodate a copious production of direct photons; Farrar and Frautschi have also pointed out that such direct photons could generate in turn, by internal conversion, an important lepton yield [7].

We report on a simultaneous measurement of the yields of single photons and of photon pairs produced at 90° in proton-proton collisions of total c.m. energies  $\sqrt{s} = 45$  and 53 GeV. We compare the rate of production of single photons to what

<sup>\*</sup> Visitor from III. Physikalisches Institut der Technischen Hochschule, Aachen, Germany.

<sup>\*\*</sup> Present address: Enrico Fermi Institute, University of Chicago, Chicago, Illinois 6063, USA.

<sup>\*\*\*</sup> Visitor from Institut für Hochenergiephysik, Heidelberg, Germany.

<sup>†</sup> Present address: Istituto di Fisica dell'Università, Bologna, Italy.

<sup>††</sup> Now at University of California, Santa Cruz, Cal. 95064, USA.

<sup>†††</sup> Visiting scientist from JINR, Dubna, USSR, on leave from Central Research Institute for Physics, Budapest, Hungary.

would be expected from  $\pi^0$  decays as measured in the same experiment from the yield of photon pairs.

## 2. Experimental set-up

The photon detector is a lead glass hodoscope located at  $90^\circ$  production angle in an intersection region of the CERN ISR. Its properties and performance have been described in detail in previous publications [3,4]. The distance to the beam intersect is 3.62 m, corresponding to a solid angle acceptance of 0.05 sr in the pp center-of-mass system. To analyse the pattern of energy distribution in the lead glass array, we reduce it to a number of clusters of connected cells with pulse height significantly above zero. On the average each cluster has more than 90% of its energy in three cells and two photon clusters can be resolved down to a 20 cm separation between photons. The energy resolution of a single cell, as measured in a 1 GeV electron beam long before the experiment, was typically  $\pm 7\%$ . The actual energy resolution of the counter as a whole was however almost twice as large in the conditions of the experiment.

The space around the beams is covered by a large acceptance magnetic spectrometer, the Split Field Magnet Facility [8], where charged particles produced in association with the lead glass trigger are detected. The corresponding data are not of direct relevance to the present study and are discussed in detail elsewhere [9].

Events were recorded when they simultaneously satisfied two conditions: an energy deposition above an adjustable threshold (usually 1.4 GeV) in the lead glass counter and the detection of two charged particles either in the SFM wire chambers or in each of two scintillation hodoscopes positioned at small angles to the beam lines. The second condition ensures that the detected photons are produced in a genuine beam-beam interaction while it may cause a loss of at most 10% to the inclusive photon spectrum.

## 3. Experimental method

The comparison of the measured single photon yield to that expected from  $\pi^0$  decays involves three operations: the measurement of the yield of  $\pi^0$ 's (identified as photon pairs with correct invariant mass), a calculation of the single photon yield expected from  $\pi^0$  decays seen by the detector (using the measured  $\pi^0$  cross section) and the measurement of the single photon yield itself. The method is free of normalization errors since photon pairs and single photons are simultaneously observed in the same experiment. However there are three potential sources of systematic biases:

(i) the identification of single photons is not constrained as that of photon pairs from  $\pi^0$  decays, for which the measured value of the invariant mass provides a clear signature.

(ii) a loss of photons would affect the pair sample more than that of singles and cause an apparent excess of single photons.

(iii) an accurate knowledge of the shape of the energy response curve of the lead glass counter is essential because a single photon detected in the counter usually carries most of the energy of its parent  $\pi^0$  (87% on the average) while photons from a resolved photon pair carry on the average half of the  $\pi^0$  energy. To illustrate this point consider a 2 GeV photon detected as a single photon. Because of the steep fall of the production spectrum its parent  $\pi^0$  is most likely to have an energy only slightly higher, say 2.2 GeV. If a 2.2 GeV  $\pi^0$  is instead detected as a resolved photon pair, each photon carries 1.1 GeV on the average. Assume now that energies are correctly measured around 1 GeV but are 5% lower than the measured values around 2 GeV. We would compare the single photon yield inferred from identified  $\pi^0$  decays at 2 GeV to observed single photon yield at an energy 5% lower, which implies a 40% apparent excess of single photons.

We briefly list the main properties of the kinematics of the two photon decay of an object with four-momentum  $(\mathbf{p}_0, E_0)$  and mass  $m_0$ . The photons have energies  $E^\pm = \frac{1}{2}E_0(1 \pm \alpha)$  and an opening angle  $\theta$  strongly peaked near its minimum value  $\theta_{\min} = 2 \tan^{-1} m_0/p_0$ . The energy asymmetry  $\alpha$  is uniformly distributed, larger asymmetries corresponding to more open pairs. For  $\alpha = 0.5$  the opening angle is only 17% higher than  $\theta_{\min}$ . In the geometry of the present experiment a  $\pi^0$  can be detected as a resolved photon pair when its laboratory energy lies between 0.9 and 3.6 GeV. The lead glass hodoscope is too small to permit simultaneous detection of both decay photons from a lower energy  $\pi^0$  while a higher energy  $\pi^0$  will sometimes appear as an unresolved photon pair. Two-photon decays of  $\eta$  mesons can only be observed above 4 GeV; but the production cross section is so low at this energy that in the present experiment  $\eta$  decays will mostly contribute to single photon events.

The effective acceptance for the detection of a 2 GeV (4 GeV)  $\pi^0$  as a resolved photon pair with  $\alpha < 0.5$  is 5.3 msr (12.7 msr).

With the above numbers in mind we restrict the transverse momentum range of the present analysis to the interval  $1.6 \text{ GeV}/c < p_t^{\text{cm}} < 3.8 \text{ GeV}/c$  ( $1.4 \lesssim E_0^{\text{lab}} \lesssim 3.2 \text{ GeV}$ ) where  $\pi^0$ 's are detected as resolved photon pairs with good efficiency. In addition we require the energy asymmetry  $\alpha$  to be smaller than 0.5, which ensures that both decay photons have energies above 350 MeV, namely in a range where the contamination from charged hadrons is very small.

#### 4. Energy calibration of the lead glass hodoscope

The lead glass hodoscope is comprised of 61 hexagonal cells; each cell is viewed by an independent phototube for which the pulse area  $\sigma$  is recorded for each event. The problem of energy calibration consists in establishing the 61 relations

$$E = f_i(\sigma), \quad i = 1, 61,$$

where  $E$  denotes the energies deposited in each cell. In the following we assume that a universal function  $f_0(\sigma)$  describes the energy responses of all cells up to a factor, namely

$$f_i(\sigma) = \lambda_i f_0(\sigma),$$

and we will comment later on the validity of this assumption.

Cell gains had been adjusted, prior to installation in the ISR tunnel, by illuminating each cell from the center of its front face with a reference light source, a small quantity of  $^{241}\text{Am}$  imbedded in a sodium iodide crystal. The energy equivalent of this reference light source had been previously measured to be 2.4 GeV for one of the lead glass cells in an electron beam at DESY. A system of light diodes [4] was used to monitor cell gains and check their constancy during the course of the experiment.

The constants  $\lambda_i$  are adjusted (up to a common factor) from the data themselves by requiring that each cell record a number of counts above 2 GeV consistent with the approximately uniform illumination expected from  $\pi^0$  decays. On the average corrections of  $\pm 9\%$  with respect to the preliminary adjustments from the reference light source are necessary. If the threshold is lowered to 1 GeV we obtain a new set of constants, identical to the first to within  $\pm 2\%$ . This gives us confidence that the assumption of shape independence for  $f_i(\sigma)$  is justified. In order to adjust the normalization factor common to all  $f_i(\sigma)$  we required that the invariant mass spectrum of photon pairs peak at the  $\pi^0$  mass. As an independent check of the relative adjustment of the  $\lambda_i$ 's we have studied the invariant mass spectra of photon pairs with one photon in a given cell and the other elsewhere in the counter. In each case we observe the peak at  $135 \text{ MeV}/c^2$  to within  $\pm 2\%$ .

To measure  $f_0(\sigma)$  at different energies we moved the lead glass counter to a smaller production angle ( $45^\circ$  in the pp center-of-mass system) where the bending power of the Split Field Magnet is 8 kGm (instead of 1.3 kGm for the  $90^\circ$  data). In that position it was possible to momentum analyse in the SFM wire chambers electrons and positrons from photon conversions in the vacuum pipe, and adjust their energy as measured in the lead glass counter. Since there was no specific particle identification we only consider positrons. This avoids mistaking antiprotons for electrons and keeps hadron contamination to a negligible level.

In order to monitor possible changes of the  $\lambda_i$  parameters when moving from one position to the other, we repeated the mass analysis of photon pairs with the  $45^\circ$  data. Distributions in the energy differences obtained from the chamber and lead glass measurements with positron data are presented in fig. 1 for four intervals of energy between 1 and 4 GeV. The widths of the curves ( $\pm 250 \text{ MeV}$  between 1 and 2 GeV) can be accounted for if the energy resolution of the lead glass counter is as large as  $\pm 14\%$ . The data are affected by radiation losses in the material of the proportional chambers (0.15 radiation lengths) which cause the energy deposited in the lead glass counter to be on the average lower than the momentum measured in the

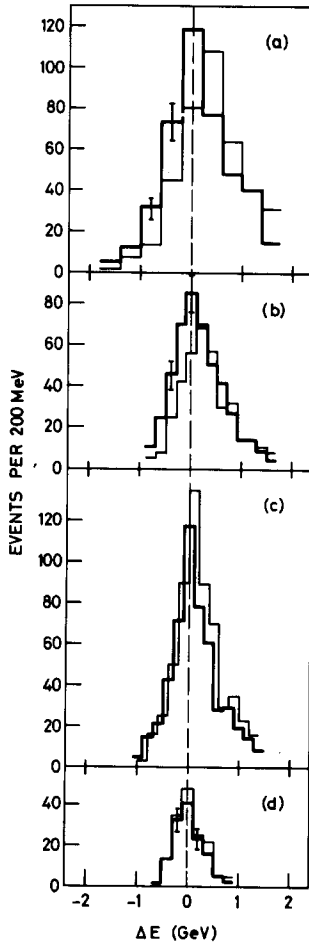


Fig. 1. Positron data. Distributions in  $\Delta E$ , the difference between the energies measured in the SFM detector and in the lead glass counter, are shown for various energy intervals. The mean energies in each interval are 3.3 GeV (a), 2.3 GeV (b), 1.7 GeV (c) and 1.2 GeV (d). Also shown (thin lines) are the same distributions for the minimum modification of the energy response curve of the lead glass counter such that the excess of single photons (see sect. 6) would disappear. A few typical error bars are indicated.

SFM detector. The high  $\Delta E$  tails in the distributions of fig. 1 can be ascribed to this effect; the positions of the maxima, however, are not expected to be affected and they were used to calculate  $f_0(\sigma)$ .

We find that the dependence of  $f_0(\sigma)$  upon  $\sigma$  (fig. 2) can be approximated by the

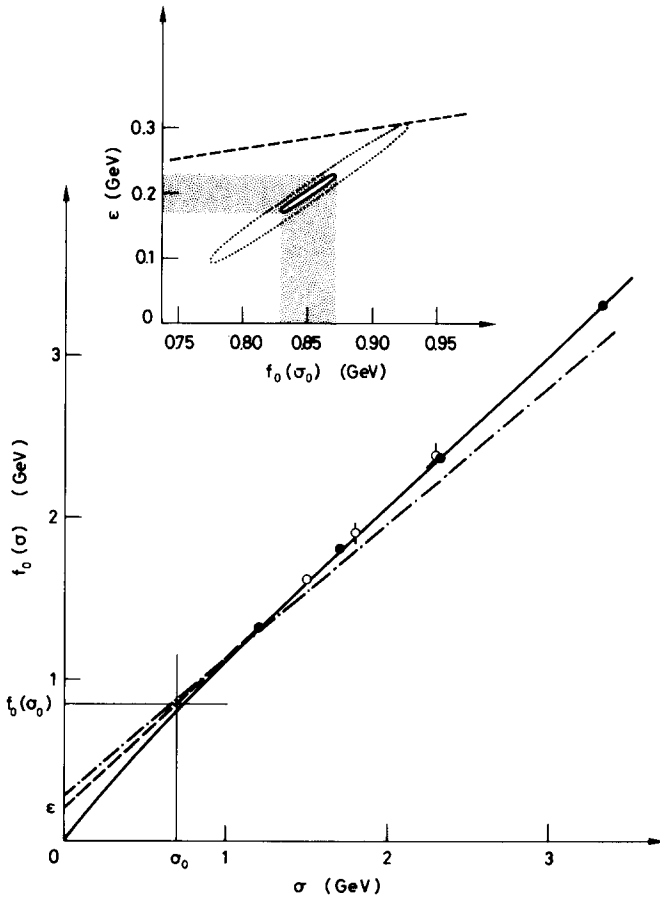


Fig. 2. Energy response of the lead glass counter. Positron data points (full circles) are shown together with the corresponding response curve (heavy line) giving  $\epsilon = 0.20 \pm 0.03$  GeV. In actual calculation the linear approximation was replaced by a parabolic dependence below 1 GeV. Also shown (open circles) are the calibration points obtained from the study of mass spectra of photon pairs (see text). While the point to point uncertainties on these data are as good as  $\pm 1.5\%$  they have been increased to  $\pm 3\%$  to account for possible differences between the responses of the lead glass counter to photons and to positrons. In the insert we show the best fit values of  $\epsilon$  and  $f_0(\sigma_0)$  to the positron data, together with the one standard deviation ellipse. The dotted line indicates the value of  $\epsilon$  and  $f_0(\sigma_0)$  which would cause the observed excess of single photons to cancel, three standard deviations away from the best fit (dotted ellipse and dash-dot line in the figure itself).

expression

$$f_0(\sigma) = f_0(\sigma_0) \frac{\sigma}{\sigma_0} + \epsilon \left( 1 - \frac{\sigma}{\sigma_0} \right).$$

We choose  $\sigma_0$  to correspond to 0.85 GeV on the average, the mean photon energy for  $\pi^0$  decays. This parametrization conveniently decouples the information on the

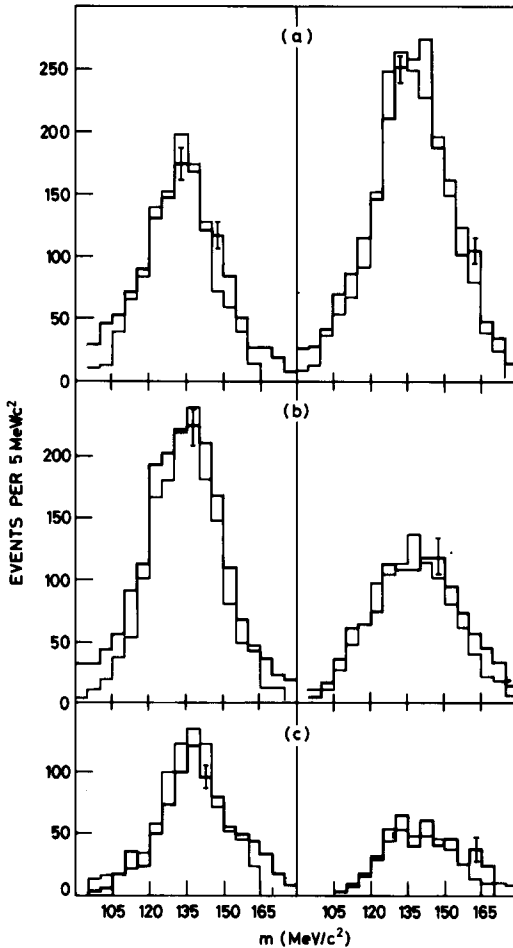


Fig. 3. Invariant mass distributions (heavy lines) of asymmetric photon pairs in the  $45^\circ$  data (left column) and in the  $90^\circ$  data (right column). The energy of one of the photons is restricted to the interval 0.6 to 0.9 GeV; that of the other photon lies between 1.2 and 1.6 GeV (a), between 1.6 and 2.0 GeV (b) or between 2.0 and 3.0 GeV (c). Monte-Carlo distributions (thin lines) are shown for comparison. A few typical error bars are indicated.

shape of  $f_0(\sigma)$  coming from the positron data, from that on the normalization coming also from the pair mass spectrum.

Considering the positron data alone, we find

$$\epsilon = 0.20 \pm 0.03 \text{ GeV},$$

and the photon pair invariant mass distribution gives for the measured  $\pi^0$  mass a value

$$m = 134.8 \pm 0.6 \text{ MeV}/c^2,$$

where the error is statistical only.

The above value of  $\epsilon$  is consistent with an estimate obtained from the response curve of the analog to digital converters used to process the phototube pulses and with the energy calibration curve previously measured for one of the cells in electron beams with energies between 0.5 and 5 GeV.

In order to gain confidence in the above study we have independently obtained an estimate of  $\epsilon$  from the energy dependence of the mass distribution of photon pairs from  $\pi^0$  decays. To this effect we consider photon pairs with one of the photons having an energy between 0.6 and 0.9 GeV and study their mass distribution for various ranges of energy of the other photon. The results are compared in fig. 3 with the results of a Monte-Carlo calculation taking into account the cell structure of the lead glass array. This must be done in some detail to correctly reproduce the relation between actual and measured impact points: cell size effects distort the steep distribution of opening angles in the vicinity of  $\theta_{\min}$ , and introduce an apparent dependence upon energy of the measured pair mass, of typically  $2 \text{ MeV}/c^2$  per GeV. The shape of the mass distributions corresponds to an energy resolution of  $\pm 13\%$  for the lead glass counter as a whole.

With this method we can adjust the mass distributions to an accuracy of  $\pm 1.5 \text{ MeV}/c^2$  and find

$$\epsilon = 0.19 \pm 0.03 \text{ GeV}$$

in agreement with the determination obtained from the positron data.

From the analyses above, we retain for  $\epsilon$  the value  $0.20 \pm 0.03$ . The corresponding uncertainty in the total single photon rate (when comparing it to that inferred from resolved photon pairs) is 10 to 15% depending upon energy. The uncertainty of  $f_0(\sigma_0)$  only affects the global energy scale and has little effect to the extent that we deal with almost exponential energy distributions.

## 5. Photon pairs: the inclusive $\pi^0$ production cross section

The distribution in energy asymmetry  $\alpha$  of photon pairs produced at  $90^\circ$  with total transverse momentum between 2 and  $3.8 \text{ GeV}/c$  is compared in fig. 4 with the

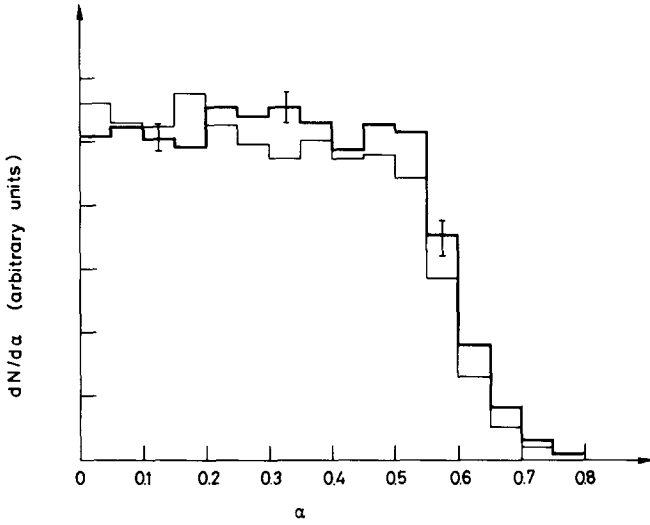


Fig. 4. The observed (heavy line) and predicted (thin line) distributions in energy asymmetry  $\alpha$  for photon pairs. Only pairs with photon energies above 400 MeV are considered. A few typical error bars are indicated.

result of a Monte-Carlo calculation. As mentioned earlier we only retain symmetric pairs with  $\alpha < 0.5$  in our sample of resolved photon pairs. In addition we require the distance between both photon impacts to be larger than 27 cm (2 cell diameters) and the invariant mass  $m$  of the photon pair to lie within the range  $50 < m < 200 \text{ MeV}/c^2$ . When more than two energy clusters are detected in the lead glass array (in 8% of the cases) we take the pair with the highest total energy. The distribution in mass for pairs selected according to the above criteria and with total transverse momentum between 2.0 and 3.8 GeV/c is shown in fig. 5. The background due to wrong pairings is estimated from 3 cluster events to be less than 2%.

Photon conversion in the vacuum pipe and in the material of the SFM detector cause a loss of events either because the conversion electrons are swept away from the lead glass counter or more commonly because of energy degradation and losses of soft electrons. From a detailed calculation simulating the conversion process and tracking the electrons in the inhomogeneous SFM field we find an event loss of  $15 \pm 3\%$ . To check the calculation we have compared the observed and calculated fractions of accepted two-photon events where a track detected in the wire chambers points to one of the lead glass clusters. We find  $4.5 \pm 1.0\%$  and  $5 \pm 1\%$  respectively.

The luminosity of the machine is measured from the rate of coincidences in the forward scintillator hodoscopes mentioned earlier to within  $\pm 5\%$  [10]. The resulting invariant cross sections are displayed in fig. 6 and listed in table 1, together with a summary of the applied corrections and systematic uncertainties. They are in good

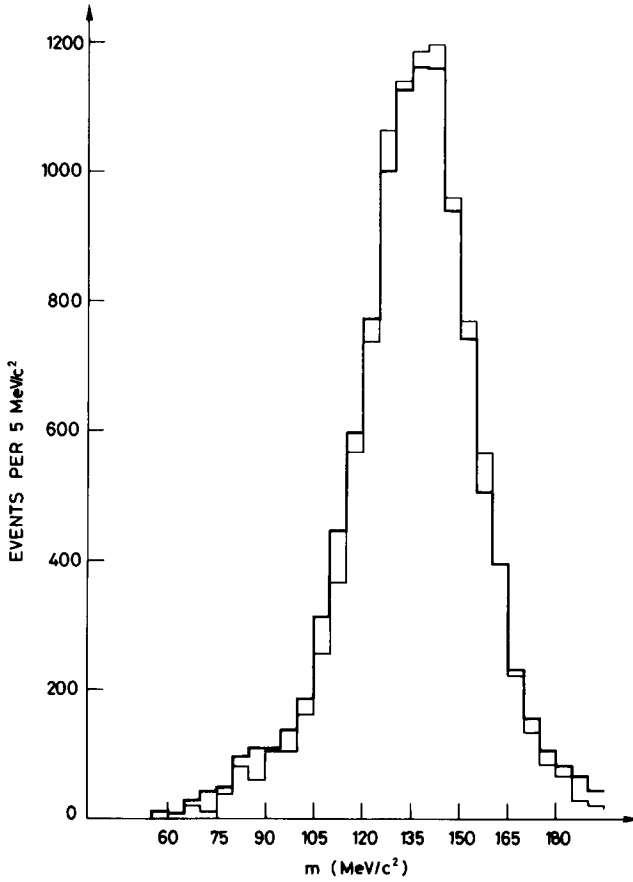


Fig. 5. Invariant mass distribution for symmetric photon pairs ( $\alpha < 0.5$ ) with c.m. transverse momentum between 2.0 and 3.8 GeV/c. The data (heavy line) are compared to the results of a Monte-Carlo calculation (thin line).

agreement with the published charged pion data of the British Scandinavian Collaboration [11].

## 6. Single photons

We retain in the sample of single photon events those where a cluster is detected in the lead glass array either alone or, in 2.8% of the cases, accompanied by an additional cluster (or clusters) of less than 100 MeV energy. This requirement helps in selecting a pure sample but the loss of single photon events accompanied by an inde-

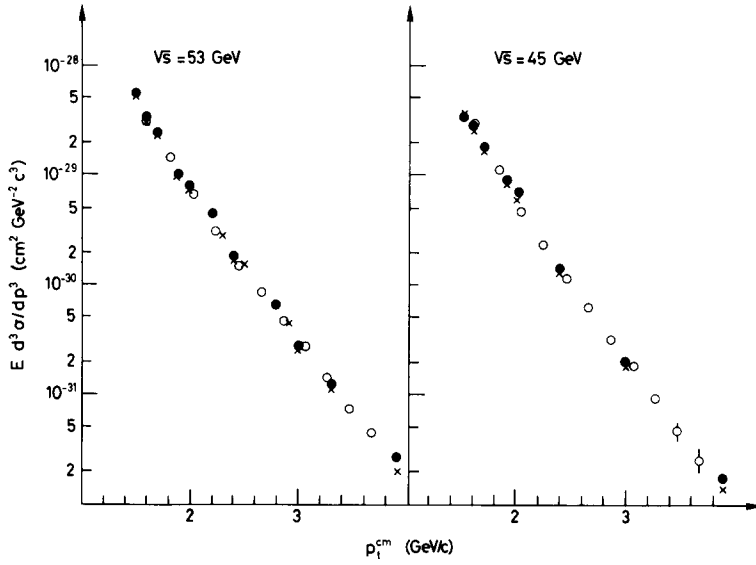


Fig. 6. Inclusive  $\pi^0$  production cross sections at  $90^\circ$  for  $\sqrt{s} = 45$  and  $53$  GeV, as measured from resolved photon pairs (open circles). Also shown are the data of ref. [11] for  $\pi^+$  (full circles) and  $\pi^-$  (crosses).

Table 1

Invariant cross sections for inclusive  $\pi^0$  production (as deduced from resolved photon pairs) at  $90^\circ$  for  $\sqrt{s} = 45$  GeV and  $\sqrt{s} = 53$  GeV

$p_t$ (GeV/c)	Invariant cross section $p + p \rightarrow \pi^0 + \dots$ ( $\text{cm}^2 \text{ GeV}^{-2} c^3$ )	
	$\sqrt{s} = 45$ GeV	$\sqrt{s} = 53$ GeV
1.6–1.8	$(2.58 \pm 0.23) \cdot 10^{-29}$	$(3.24 \pm 0.30) \cdot 10^{-29}$
1.8–2.0	$(9.61 \pm 0.71) \cdot 10^{-30}$	$(1.26 \pm 0.10) \cdot 10^{-29}$
2.0–2.2	$(3.91 \pm 0.26) \cdot 10^{-30}$	$(5.79 \pm 0.38) \cdot 10^{-30}$
2.2–2.4	$(1.84 \pm 0.13) \cdot 10^{-30}$	$(2.96 \pm 0.20) \cdot 10^{-30}$
2.4–2.6	$(1.00 \pm 0.74) \cdot 10^{-30}$	$(1.58 \pm 0.11) \cdot 10^{-30}$
2.6–2.8	$(4.90 \pm 0.40) \cdot 10^{-31}$	$(8.16 \pm 0.59) \cdot 10^{-31}$
2.8–3.0	$(2.78 \pm 0.25) \cdot 10^{-31}$	$(4.95 \pm 0.38) \cdot 10^{-31}$
3.0–3.2	$(1.59 \pm 0.16) \cdot 10^{-31}$	$(2.81 \pm 0.24) \cdot 10^{-31}$
3.2–3.4	$(8.14 \pm 0.99) \cdot 10^{-32}$	$(1.41 \pm 0.14) \cdot 10^{-31}$
3.4–3.6	$(4.11 \pm 0.63) \cdot 10^{-32}$	$(7.13 \pm 0.83) \cdot 10^{-32}$
3.6–3.8	$(2.43 \pm 0.47) \cdot 10^{-32}$	$(4.61 \pm 0.65) \cdot 10^{-32}$

The data have been corrected for background ( $-2\% \pm 1\%$ ) and for conversion losses ( $+15\% \pm 3\%$ ). In addition to the quoted uncertainties, systematic errors due to acceptance calculation and to luminosity measurements amount to  $\pm 5\%$  each.

pendent cluster must be corrected for. From the rate of occurrence of symmetric photon pairs accompanied by a third cluster we expect this loss to be of the order of 8%. This estimate is consistent with what we infer from the observed number of asymmetric ( $\alpha > 0.5$ ) photon pairs. In applying the correction to the data we implicitly assume that two-particle angular correlations are the same for  $\pi^0$ 's and for photons from other sources.

We also correct for conversions in the material between the interaction region and the lead glass counter, as we did for photon pairs. They cause an event loss of 5 to 10% depending upon energy, smaller than in the case of pairs. We can again compare the observed and calculated fractions of events with a track detected in the SFM wire chambers and pointing to a cluster in the lead glass counter. Electrons and positrons are expected to contribute 1.5% each. In fact we observe 2% positive tracks but a larger fraction, 6%, of negative tracks. We tentatively attribute the excess to antiprotons which may deposit much more than their kinetic energy when they annihilate in the lead glass. In support to this interpretation we observe that the corresponding clusters have a larger spatial extension (69% of the cluster energy is contained in a single cell instead of 80% for photons). This brings up the question of the antineutron contamination, over which we have no direct control since antineutrons leave no track in the SFM wire chambers. The antineutron contamination is not simply related to that of antiprotons because the presence of magnetic field and of material between the interaction vertex and the lead glass counter affect differently the  $\bar{n}$  and  $\bar{p}$  momentum spectra\*. We estimate that, due to this effect, the antineutron contamination may be as much as twice as large as that from antiprotons, if we assume that both particles are produced with the same cross section. This estimate, obtained from a calculation taking into account the observed  $\bar{p}$  spectrum, the SFM magnetic field and the slowing down of antiprotons in the vacuum chamber and in the SFM detector, neglects possible differences between the response of the lead glass counter to  $\bar{n}$  and  $\bar{p}$  (due, for example, to the fact that  $\bar{n}$  annihilate deeper in the glass and closer to the phototube than  $\bar{p}$  do). This can be particularly important at lower momenta where, in addition, the calculation of the efficiency of the SFM chambers to detect antiprotons is less reliable. For this reason we restrict the range of the analysis of single photon events to momenta larger than  $p_t^{\text{cm}} = 2.8 \text{ GeV}/c$ , above which value the contamination of  $\bar{p}$  and  $\bar{n}$  with  $p_t^{\text{lab}} < 0.5 \text{ GeV}/c$  is negligible. In this high momentum range we calculate the contamination of  $\bar{n}$  to be about 11% of the whole single photon yield. Comparison with a Monte-Carlo calculation describing the annihilation process in the glass and with measurements by the CCR Collaboration [5] of the response of lead glass to antiprotons of 1 and 2 GeV/c momentum give us confidence that the above estimate is reliable.

We have carefully investigated several distributions of the single photon sample in order to gain additional confidence in its purity. Among those are the lateral extension of the shower and its position in the lead glass counter, the time difference

\* We are very much indebted to L. Di Lella who brought this point to our attention.

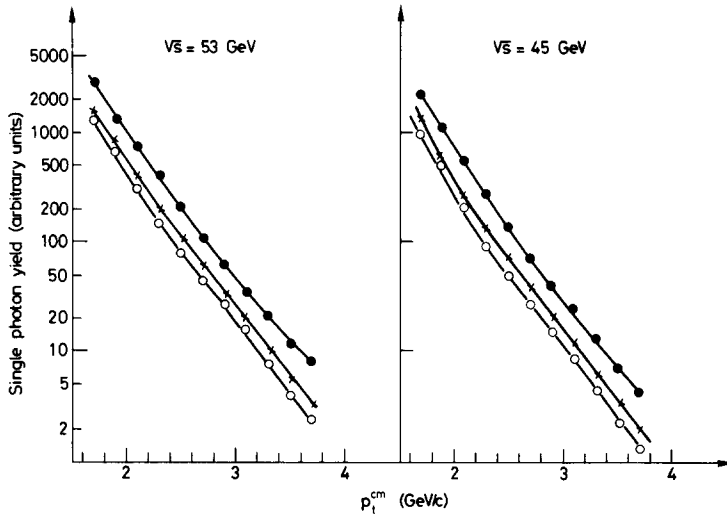


Fig. 7. Single photon yields uncorrected for antineutron contamination at  $90^\circ$  for  $\sqrt{s} = 45$  and  $53$  GeV. The observed distributions (full dots) are compared to that inferred from the resolved photon pair data (open circles). The latter are also shown after addition of the contribution from  $\eta \rightarrow \gamma\gamma$  decays (crosses).

between the lead glass pulse and the SFM wire chamber pulses (which shows a negligible accidental contribution) and the distribution of track vertices which were all found consistent with the corresponding distributions in the photon pair sample.

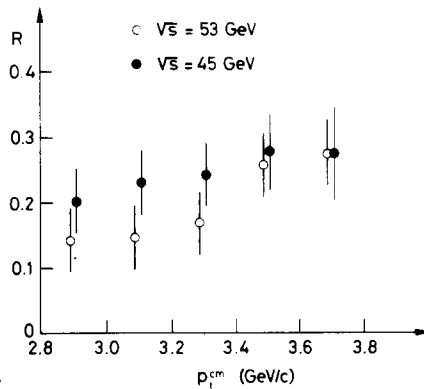


Fig. 8. The ratio  $R$  between the excess of single photons (corrected for antineutron contamination) not accounted for by  $\pi^0$  and  $\eta$  decays and the  $\pi^0$  yield measured from resolved photon pairs as a function of transverse momentum for  $\sqrt{s} = 45$  and  $53$  GeV. Error bars do not include the systematic uncertainty on the energy calibration of the lead glass counter (see text).

Table 2  
Single photon data

I	Observed single photon yield	
	Single photon events	$0.462 \pm 0.008$
	Conversion losses	$+0.032 \pm 0.009$
	Events with an independent second photon	$+0.037 \pm 0.009$
	Antinucleon contamination	$-0.077 \pm 0.046$
		$0.455 \pm 0.053$
II	Single photon yield from $\pi^0$ and $\eta$ decays	
	$\pi^0 \rightarrow \gamma\gamma$	$0.192 \pm 0.006$
	$\eta \rightarrow \gamma\gamma$	$0.062 \pm 0.011$
	Uncertainty in acceptance calculation	$\pm 0.013$
		$0.255 \pm 0.018$
III	Excess of single photons	
	$\gamma/\pi$ ratio	$0.20 \pm 0.06$
	Uncertainty on energy response	$\pm 0.07$

Data are integrated over both values of  $\sqrt{s}$  (45 and 53 GeV) and over  $p_t^{\text{cm}}$  between 2.8 and 3.8 GeV/c. All numbers are given as fractions of the  $\pi^0$  production cross section in the same range of  $p_t^{\text{cm}}$ .

We compare in fig. 7 the single photon yield uncorrected for  $\bar{n}$  contamination to that inferred from the photon pair sample. A large excess, typically 57% of all single  $\gamma$ 's, is observed at all values of  $p_t^{\text{cm}}$  and  $\sqrt{s}$ .

Radiative decays of particles other than  $\pi^0$ 's contribute to this excess. The largest contribution is expected from  $\eta \rightarrow \gamma\gamma$  decays, for which the inclusive production cross section has been measured in previous experiments [2,3], in the same range of  $p_t^{\text{cm}}$ ,  $\sqrt{s}$  and  $\theta$ . This however contributes only 12% (fig. 7) leaving a fraction of 45% of the single photon spectrum unexplained. Radiative decays from other known particles, such as  $\omega$  [9] and  $\eta'$ , are unlikely to account for such an excess.

The ratio between the single photon yield corrected for antineutron contamination in excess to that from  $\pi^0$  and  $\eta$  decays and the  $\pi^0$  yield itself is displayed in fig. 8 in the momentum interval  $2.8 \text{ GeV}/c < p_t^{\text{cm}} < 3.8 \text{ GeV}/c$  and a summary of corrections and systematic uncertainties is given in table 2. It typically amounts to 20% for both values of  $\sqrt{s}$ . To quote an uncertainty on this number we separate that coming from the energy response curve, which amounts to  $\pm 7\%$ , from that coming from all other sources, including statistics, and which amounts to  $\pm 6\%$ . While this is the first time that a copious production of single photons is mentioned in proton-proton collisions, it had previously been reported in a large  $p_t$  photoproduction experiment [12].

## 7. Conclusion

We have measured inclusive  $\pi^0$  production from identified  $\pi^0 \rightarrow \gamma\gamma$  decays at  $90^\circ$  between 1.6 and 3.8 GeV/c transverse momentum.

We have observed a large and significant production of large transverse momentum photons which cannot be explained with  $\pi^0$  and  $\eta$  decays, and which amounts to about 20% of the  $\pi^0$  production in the 2.8 GeV/c to 3.8 GeV/c range.

The geometry of the present experiment was more favourable than others [2,3], in that it permitted comparison of the single photon spectrum to that inferred from pairs in a higher range of transverse momentum than had been previously possible.

However the experiment was not specifically designed to detect single photons, but to study the structure of events with a large transverse momentum  $\pi^0$  produced at  $90^\circ$  [9]. In particular the lead glass detector was primarily intended to be used as a triggering counter and no detailed study of its energy response and resolution had been made at the time of the experiment. We have discussed in detail possible systematic biases in the course of the presentation of the data. An important one is due to the uncertainty on the shape of the energy response of the lead glass counter. In terms of the parameter  $\epsilon$ , which describes its deviation from linearity, and which we measured to be

$$\epsilon = 0.20 \pm 0.03 \text{ GeV} ,$$

we find that the observed excess of single photons would disappear if we had instead  $\epsilon = 0.29$ , three standard deviations away from the measured value. In addition the data suffer an antineutron contamination, over which we have little direct control and we must rely upon calculation to correct for it.

## References

- [1] D.C. Carey et al., Phys. Rev. Letters 32 (1974) 24; 33 (1974) 327.
- [2] F.W. Büsser et al., Phys. Letters 46B (1973) 471; 51B (1974) 306, 311; 53B (1974) 212; 55B (1975) 232.
- [3] K. Eggert et al., Nucl. Phys. B98 (1975) 49.
- [4] M. Holder et al., Nucl. Instr. 108 (1973) 541.
- [5] J.S. Beale et al., Nucl. Instr. 115 (1974) 235.
- [6] G.R. Farrar and S.C. Frautschi, Phys. Rev. Letters 36 (1976) 1017; C.O. Escobar, Nucl. Phys. B98 (1975) 173.
- [7] B.G. Pope, Rapporteur talk at Int. Conf. on high-energy physics, Palermo, Italy, 23–28 June 1975.
- [8] R. Bouclier et al., Nucl. Instr. 115 (1974) 235; 125 (1975) 19.
- [9] P. Darriulat et al., Nucl. Phys. B107 (1976) 429.
- [10] K.R. Schubert, private communication; we are grateful to the CHOV Collaboration who installed and calibrated the beam monitor hodoscopes at the SFM facility.
- [11] B. Alper et al., Nucl. Phys. B100 (1975) 237.
- [12] D.O. Caldwell et al., Phys. Rev. Letters 33 (1974) 869.